J. Webster (ed.), *Wiley Encyclopedia of Electrical and Electronics Engineering*

FOCUSED ION BEAMS IN SEMICONDUCTOR MANUFACTURING

When an energetic ion is incident on a solid surface, a number of potentially useful phenomena occur. As shown in Fig. 1, they are ion implantation, ion damage (disruption of the crystal structure), sputtering (removal of substrate atoms), secondary-ion emission, secondary-electron emission, and ion-induced surface reactions. Figure 1 shows a single point beam of ions incident on the substrate. However, in semiconductor device fabrication, many of these processes are used with a broad beam with which the entire wafer is simultaneously exposed to a flux of ions. Patterning of this flux is achieved by having part of the surface covered by a film, usually a resist. Namely, the surface is covered with a resist that is exposed by, say, UV light in a very fine pattern (nowadays, routinely down to 250 nm minimum dimensions) and developed to leave the surface partly bare and partly covered. Ions can be used to remove material preferentially from the uncovered areas by sputtering or by induced chemical reaction, or ions can be implanted into the substrate to alter its properties. The same lithographic process is also used to define metal conductors on the surface or to pattern insulating films to make the complex, multilayered ultrafine mosaic of transistors and conductors that make up integrated circuits.

That a finely focused ion beam that can be precisely deflected over a surface would be useful in semiconductor device fabrication was demonstrated as early as 1972 (1). The novel feature is that the fabrication steps that are carried out in conventional fabrication using lithography to pattern the ion dose can now be done by steering a focused point beam over the surface. This is, of course, a very slow process and will not replace conventional fabrication steps, but the fact that it is maskless and resistless can be useful in special cases as we will discuss later. In the first demonstrations, researchers at Hughes Laboratories put lenses in an ion-implanter beam and were able to do microfabrication at dimensions of micrometers, which was, at that time, the state of the art for integrated-circuit fabrication. However, this ion source was not bright, that is, not well collimated, and the current density in the focal spot was only of order 10^{-4} A/cm^2. With the discovery and development of the liquid metal ion source (2 to 4) and its installation in an ion column, a beam of 100 nm diameter and 1 A/cm^2 current density was already demonstrated in 1979 (5). Since then, various applications have been explored and continue to be explored in research laboratories. A number of these have proven to be useful in the microelectronics industry and have spurred further development of the machinery so that now beam diameters below 10 nm and current densities of 10 A/cm^2 are achieved. In this article we will mainly focus on the industrially important applications, but first we will discuss the machinery and some of the fundamental ion–surface interactions.

Focused Ion-Beam Machines

The focused ion beam systems in use can be regarded as being composed of four parts: the ion sources, the ion optical column, the sample chamber x–y stage, and the control electronics. The first three of these are shown schematically in Fig. 2. The control electronics supplies the needed voltages to the source, to the ion optical elements in the column, to the beam deflection plates, and to the x–y stage. Programmed computer control of

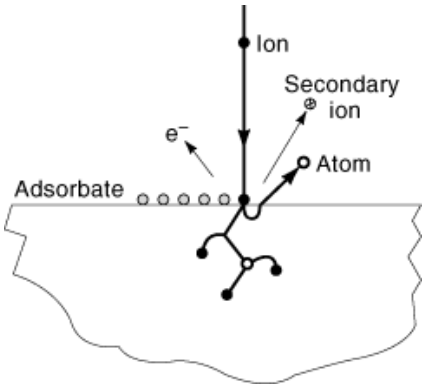

Fig. 1. Illustration of ion–solid interactions. The incident energetic ion penetrates into the solid and is implanted. It will displace lattice atoms along the way creating damaging. Surface atoms (or ions or ionized clusters) will be sputtered off and chemical reactions may be induced, involving adsorbed gas molecules. In addition secondary electrons are emitted.

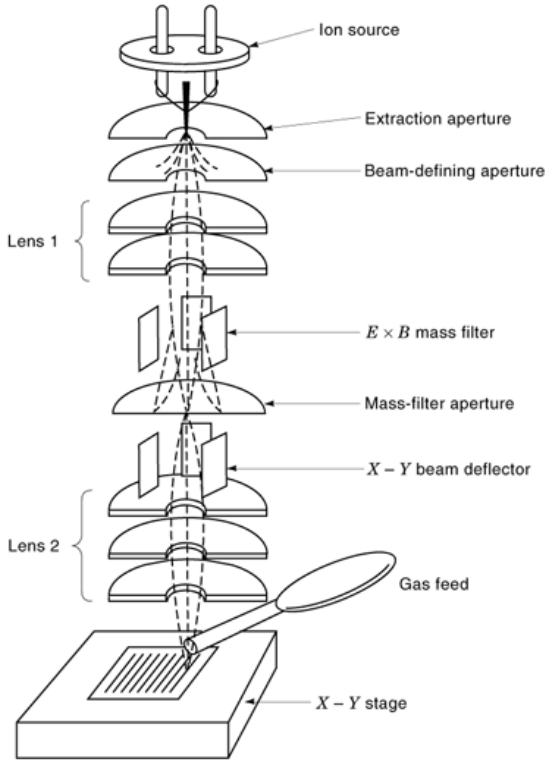

Fig. 2. Schematic of the main parts of a focused ion-beam (*FIB*) system. The liquid-metal ion source provides a "point" source of ions that is focused on to the sample on the x–y stage. The ion beam passes through electrostatic lenses consisting of two or more washerlike disks with high voltage between them. If an alloy source is used, then the system has an $\boldsymbol{E} \times \boldsymbol{B}$ filter. If Ga^+ ions only are used, which is most often the case, then the $\boldsymbol{E} \times \boldsymbol{B}$ filter is omitted. The gas feed is a fine capillary tube that creates a local gas ambient where the ion beam is incident and is used for ion-induced deposition or ion-assisted etching. In some cases an electron gun is also incorporated which aims low-energy electrons at the sample to avoid charging of insulating samples.

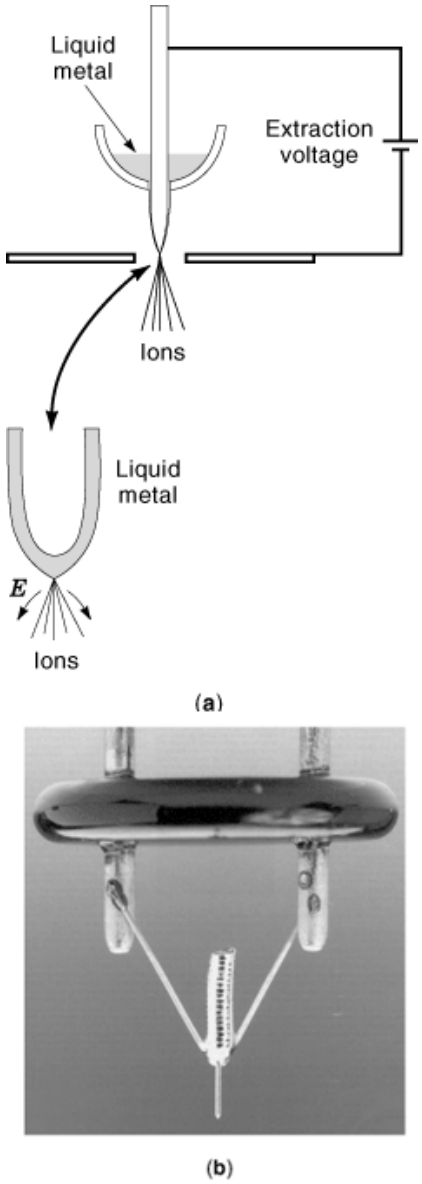

Fig. 3. (a) Schematic of a liquid-metal ion source. The electric field between the extraction aperture and the source tip pulls the liquid metal into a sharp cusp from which the ions are emitted. (b) A photograph of a liquid-metal ion source. The ceramic disk that holds the electrodes is a little less than 1 cm diameter. Current is passed through the wires from the electrodes to heat the liquid metal held in the coil by surface tension.

the beam deflection and dose permit the desired operations to be carried out. More extensive discussions of focused ion-beam systems may be found in the literature (6 to 8).

The Ion Source. The ion source consists of a tungsten needle that has a film of liquid metal flowing down its shank (Fig. 3). The liquid metal is provided by some kind of heated reservoir. For example, it can be a loop of tungsten wire that has a current passing through it (as in Fig. 3) or it can be a heated graphite cup with

the tungsten needle protruding through the bottom. In either case, the tungsten needle faces an extraction aperture, a washer with a hole in the middle concentric with the needle tip (Fig. 2). A positive voltage is applied to the needle relative to the extraction aperture. The liquid metal on the tip of the needle is pulled into a cusp and ions are emitted from the tip of this cusp. For optimum source operation, the extracted current is in the 1 μA to 3 μA range. The metal most often used is Ga because of its low melting temperature, its low vapor pressure, and the fact that the ions are emitted singly ionized. The ion current emanates from the tip in a cone of 20° to 30°.

Ion Optical Column. The overall function of the ion optical column is to focus the ions emitted from the "point" source to a point on the sample. The first element in the ion optical column is the beam-limiting aperture, which accepts only a few milliradians of the cone of current emitted by the source. This corresponds to a current of a few tens of picoamps to a few nanoamps. The current has to be limited because the electrostatic ion lenses are "ideal" only near the axis. Trying to pass more current through the column simply enlarges the beam focal spot on the sample. In fact, over part of the range of beam currents available, the current density in the focal spot is constant, so that, for example, doubling the current will increase the diameter of the focal spot by $\sqrt{2}$. The beam spot on the sample is approximately Gaussian, that is, the current density as a function of radius is proportional to $\exp(-r^2/2\Phi^2)$, where Φ is the half-width of the beam spot where the current density is 61% of the peak value (at $r = 0$).

The lenses as seen in Fig. 2 consist of concentric washerlike elements precisely machined, highly polished, and precisely aligned. A high voltage is applied between the elements so that, for example, after passing through the first lens the ions may have 30 keV to 50 keV of energy. The lowest lens is often a symmetric enizel lens, that is, it focuses the beam but does not change its energy since the outer two electrodes are grounded while the central electrode has a voltage applied. The beam is deflected in x and y directions by applying transverse electric fields using deflection plates. Since the beam deflections are usually small, the deflection can be carried out above the final lens, thus permitting shorter working distances and hence smaller beam diameters. Often double deflection is used above the lens so that the beam passes through the center of the lens independent of the degree of deflection, but its angle with respect to the axis is proportional to the deflection. A blanker is used to turn the ion beam off. This is done by having another pair of deflection electrodes that apply a transverse electric field when needed and deflect the beam to one side so that it fails to pass through a downstream aperture.

Mass Separator. If ions other than Ga are desired, an alloy source is used. Systems with alloy sources are usually used in research, for example, to implant dopants into silicon (boron or arsenic) or into gallium arsenide (berylium or silicon). These dopants can be incorporated into alloy sources (e.g., Au/Be/Si or Pd/As/B). In order to focus only the desired ion, the other constituents of the alloy source have to be filtered out. This is accomplished by use of a filter consisting of crossed electric and magnetic fields perpendicular to the axis, a so-called $\boldsymbol{E} \times \boldsymbol{B}$ filter.

Control Electronics. The voltages that need to be applied to the lenses are determined by the energy needed for the ions incident on the sample and by the desired focal planes. For implantation systems that use $\boldsymbol{E} \times \boldsymbol{B}$ filters the maximum overall column accelerating potential is usually 150 kV. (Some ion species are available doubly ionized so that 300 keV of incident ion energy is available.) Usually the final energy is adjustable, but lowering the voltage increases the beam diameter of the focal spot on the sample.

The systems that use Ga ions only, which are, by far, the most widely used, are designed to operate at maximum voltages in the 30 keV to 50 keV range and do not need an $\boldsymbol{E} \times \boldsymbol{B}$ filter.

Both kinds of systems are in all cases, except for home-built laboratory systems, operated under computer control. The computer controls the lens voltages, helps to establish optimum focus, scans the beam to deliver a precise dose to a precisely defined area, moves the sample stage, and controls the various peripheral systems such as vacuum pump and load locks.

Sample Chamber and *x–y* Stage. The ion column, which has its own vacuum pump (usually an ion pump) is connected to a sample vacuum chamber and the pion beam enters the sample chamber through a

Fig. 4. A photograph of a focused ion-beam system showing the ion column mounted on a vacuum chamber.

small hole, permitting a pressure difference to exist between the two. The sample is about 1 cm below the tip of the ion column. The ion beam can be deflected over fields of about 300 μm $\times$ 300 μm. If a very precise deflection is needed, then a smaller field size is used, since some distortion may occur near the perimeter of large fields.

Clearly, if the beam diameter of order 10 nm is used, then beam motion due to acoustic vibration or due to electronic noise has to be less than 10 nm. Thus, the x–y stage, the chamber, and the column are built mechanically very rigidly, and care is taken to limit ambient electromagnetic interference and noise in the voltages supplied to the column.

The fabrication processes that make use of ion-induced surface chemistry require a precursor gas to be supplied to the surface. This is accomplished by a capillary feed consisting of a fine $\sim$1 mm diameter tube pointed close to the area where the ion beam scans. Thus, the gas pressure on the sample at the mouth of the tube is in the 1 mTorr to 20 mTorr range, while the pressure in the chamber is in the 10^{-5} Torr to 10^{-6} Torr range. The type of gases fed to the surface will be discussed later.

Many systems also have a built-in electron flood gun that directs a beam of electrons to the area addressed by the ion beam so that the surface does not charge up. This is important when highly insulating samples such as quartz masks need to be milled. A photograph of a typical focused ion beam (*FIB*) system is shown in Fig. 4.

Fundamental Processes

Of the various ion–surface interaction processes illustrated in Fig. 1, the ones most often used are (a) secondary-electron emission; (b) milling, that is, material removal by sputtering, and (c) ion-induced surface chemistry, which is deposition from a precursor gas, or accelerated material removal by etching with a reactive precursor gas.

Secondary-Electron Emission. Secondary-electron emission is universally used to image with the ion beam in the scanning ion microscope mode. This is completely analogous to a scanning electron microscope (*SEM*), except that an ion beam instead of an electron beam is scanned. The secondary electrons are generally collected by a channel electron multiplier, and the signal is used to modulate the intensity on a cathode ray tube. Needless to say, the imaging process erodes the surface. However, if image capture is used instead of repeated scanning, the erosion can be quite minimal, on the order of a monolayer. Imaging is useful, for example, in locating the area to be milled and in examining the outcome of a milling process.

Milling. An energetic ion incident on a solid loses its energy by scattering the electrons in the solid and by scattering the lattice atoms. (These energy losses are also referred to as electronic stopping power and nuclear stopping power.) The electron scattering is a smooth continuous process and would by itself lead to a uniform slowing of the ion with negligible change in direction. The scattering against the atoms is a stochastic process and leads to displacement of lattice atoms from their normal sites. The scattered atoms have enough energy to scatter other atoms leading to the so-called collision cascades. This has been modeled by a Monte Carlo technique called *TRIM* (transport of ions in matter) and developed into a widely used computer program (9). When a collision cascade atom reaches the sample surface, enough energy can be imparted to it to exceed the binding energy, and atoms are sputtered from the surface. The number of atoms removed per incident ion is called the sputter yield. The TRIM calculation is quite accurate in predicting the sputter yield over a wide range of ion masses and energies (10). Various experimental yield measurements, particularly with noble-gas ions, are available (11).

For *FIB* milling the sputter yield due to Ga^+ ions is of interest. Some of the measured values are shown in Table 1. There appear to be differences in the measured yield values, which may be due to one or more of the following effects, which may alter the material removal rate:

(1) *Scan Speed.* Yield is usually measured by raster scanning the focused ion beam over some rectangle on the surface and then measuring the depth of the pit produced. If the raster scan is slow and the thickness of the layer removed per scan is comparable to the beam diameter, then locally under the beam the ions will not be normally incident on the surface. This will lead to an increase in yield (12), since the sputter yield has been observed to increase as the angle of incidence changes from normal toward grazing incidence (13). Thus, the yield that is measured will depend on the scan rate unless the scan rate is fast.

(2) *Orientation of Crystal Axis.* The penetration of ions into a crystal depends on the orientation of the crystal axis relative to the ion beam. Thus, if the beam is oriented along a crystal symmetry axis, the atoms will appear to be in rows with open spaces between them. Thus, the ion will penetrate deeper before scattering, due to this so-called channeling effect. The ions that channel will produce fewer collision cascades at the surface and will have a lower sputter yield. If a polycrystalline sample is milled, the dependence of yield on orientation will lead to different milling rates for different grains. This will result in an apparent roughening of the surface and a difficulty in determining a milling yield (see Fig. 5).

(3) *Redeposition.* When a shallow pit is milled at normal incidence with a rapid scan, the sputtered atoms will predominantly leave the substrate. However, when a deep pit is milled with a single scan, the sputtered atoms will tend to fill in the region that has just been milled. This has been observed and modeled as shown in Fig. 6. Unless care is taken, redeposition can also affect the measured sputter yield.

Table 1. Ion Milling Yields for Focused Ga (Atomic Mass 69) and Broad-Beam Kr Ions (Atomic Mass 84)

Substrate	Ion	Energy (keV)	Yield (atoms/ion)	Reference
Si	Ga^+	30	3.1±0.8	(*a*)
Si	Ga^+	30	2.1	(*b*)
Si	Ga^+	25	2.6	(*c*)
Si	Ga^+	25	3.9±0.4	(*d*)
Si	Kr^+	25	3.1	(*e*)
Au	Ga^+	100	32	(*f*)
Au	Ga^+	40	15.7±1.3	(*g*)
Au (plated)	Ga^+	25	18±3	(*d*)
Au (evap.)	Ga^+	25	23±5	(*d*)
Au	Kr^+	25	20	(*e*)
		45	28	
W (RF sputt.)	Ga^+	25	5±0.7	(*d*)
W	Kr^+	22	4.1	(*e*)
SiO_2	Ga^+	68	2.0*	(*h*)
SiO_2	Ga^+	25	0.84*	(*d*)
SiO_2	Ga^+	30	0.85*	(*b*)

[a] H. Yamaguchi, *J. Phys. Colloq. C6,* **48** (Suppl. 11) C6-165, 1987.
[b] D. Santamore et al., *J. Vac. Sci. Technol.,* **B15:** 6, 1997.
[c] J. G. Pellerin et al., *J. Vac. Sci. Technol.,* **B7:** 1810, 1989.
[d] X. Xu et al., *J. Vac. Sci. Technol.,* **B10:** 2675, 1992.
[e] H. H. Anderson, and H. L. Bay, Sputter yield measurements, in R. Behrisch (ed), *Sputtering by Particle Bombardment I, Physical Sputtering of Single Element Solids,* Berlin: Springer, 1981, p. 145.
[f] P. K. Muller and H. C. Petzold, *SPIE,* **1263:** 12, 1990.
[g] P. G. Blauner et al., *J. Vac. Sci. Technol.,* **B7:** 609, 1989.
[h] J. Melngailis et al., *J. Vac. Sci. Technol.,* **B4:** 176, 1986.
* molecules/ion

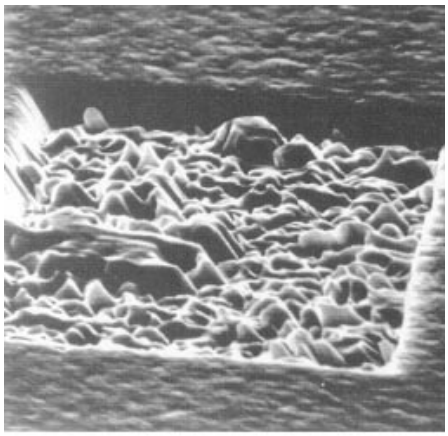

Fig. 5. Gold film in which a pit has been *FIB* milled. The apparent roughening of the bottom of the pit is due to the fact that individual grains mill at different rates depending on orientation. (From Ref. 13.)

(4) *Angle of Incidence.* The sputter yield increases as the angle of incidence between the beam and the sample departs from normal. This is illustrated in Fig. 7 and is important when one deliberately tilts the sample with To mill a desired structure in practice, these effects usually need to be considered.

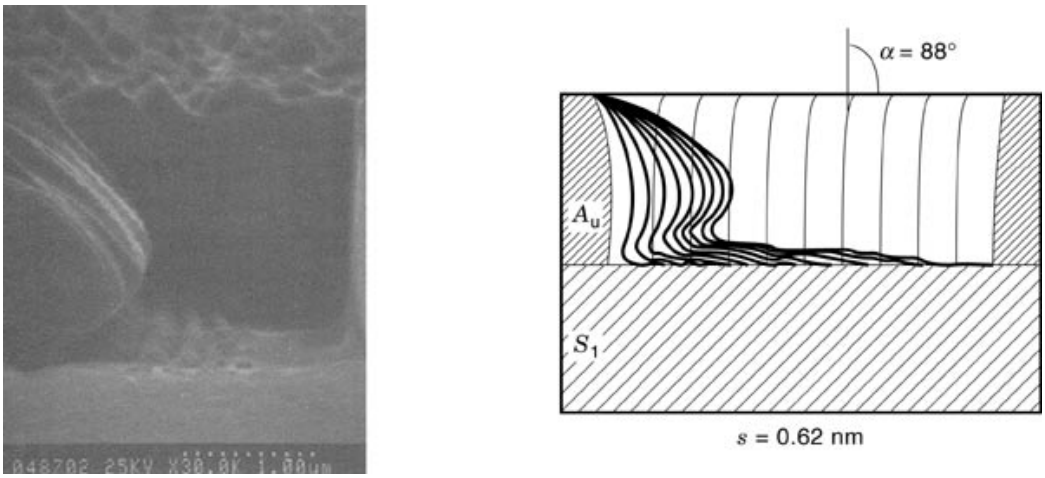

Fig. 6. On the right, the simulation of the redeposition occurring when a deep pit is milled in a single pass of the beam from left to right. On the left, the observed redeposition P. K. Müller and H. C. Petzold, *SPIE*, *1263*: 12, 1990.

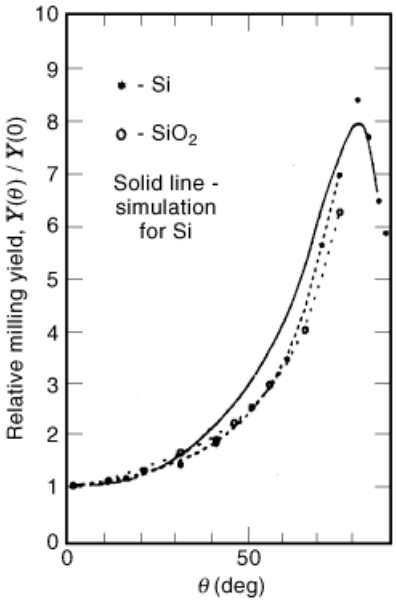

Fig. 7. From Ref. 13. Relative milling yield versus angle of incidence. The solid lines represent the results from a Monte Carlo simulation (TRIM). The dotted lines serve only to guide the eye. Results for SiO_2 were obtained by milling a quartz fiber with 35 keV Ga^+ at a beam current of 100 pA and an average current density of 2.9 pA/m^2. Milling conditions for the rest: beam, 25 keV Ga^+, beam current, 283 pA; dwell time, 0.3 s/pixel; average current density, 7 pA/m^2 for W and Si, 2.9 pA/(μm^2) for Au.

Ion-Induced Deposition. To complement the material removal by ion milling, a method of material addition is useful. In ion-induced deposition a precursor gas, often an organometallic, is directed to the surface by a capillary tube as shown in Fig. 2. The gas molecules adsorb on the surface where the incident ion beam causes them to dissociate, leaving the metal constituent as a deposit. Clearly the ion beam also mills the

Table 2. Ion-Induced Deposition

Gas	Ion, Energy	"Yield" (atoms/ion)	Deposit Composition	Resistivity (Ω · cm)	Reference
WF_6	Ar^+, 500 eV and 2 keV		W:F:C 93.3:4.4:2.3	15	(*a*, *b*)
$W(CO)_6$	Ga^+, 25 keV	2	W:C:Ga:O 75:10:10.5	150–225	(*c*)
$C_7H_5F_6O_2Au$	Ga^+, 40 keV (room temp.)	3–8	Au:C:Ga 50:35:15	500–1500 (bulk Au = 2.44)	(*d*)
	Ga^+, 40 keV at 120°C	3	Au:C:Ga 80:10:10	3–10	(*e*)
$C_9H_{17}Pt$	Ga^+, 35 keV	0.2–30	Pt:C:Ga:O 45:24:28:3 25:55:19:2	70–700 (Bulk Pt = 10.4)	(*f*)
$(CH_3)_3NA1H_3$	Ga^+, 20 keV	4–6	Al:Ga:C:N	900	(*g*)
Cu(hfac)TMVS	Ga^+, 25–35 keV	10–30	Cu:C 60:50 (25°C) 95:5 (100°C)	100 5	(*h*)
TMOS + O_2	Si, 60 kV	1 mol/ion	SiO_x	2.5×10^6	(*i*)
OMCTS + O_2	Ga, 50 kV		Si:O:Ga 27:56:17	1.2×10^7	(*j*)
TEOS	Ga, 30 kV			10^8	(*k*)
PMCPS	Ga, 30 kV		SiO_x	8×10^{11}	(*l*)

* The resistivity of the FIB deposited oxides is nonlinear and depends on the applied electric field. The values quoted should be viewed as very approximate and cannot be directly compared since they were not measured at the same applied electric field.

[a] Z. Xu et al., *J. Vac. Sci. Technol.*, **B7:** 1959, 1989.
[b] K. Gamo and S. Namba, *Proc. 1989 Intern. MicroProcess Conf.*, p. 293.
[c] D. K. Stewart, L. A. Stern, and J. C. Morgan, *SPIE*, **1089:** 18, 1989.
[d] P. G. Blauner et al., *J. Vac. Sci. Technol.*, **B7:** 609, 1989.
[e] P. G. Blauner et al., *J. Vac. Sci. Technol.*, **B7:** 1816, 1989.
[f] T. Tao et al., *J. Vac. Sci. Technol.*, **B8:** 1826, 1990.
[g] M. E. Gross, L. R. Harriott, and R. L. Opila, *J. Appl. Phys.* **68:** 4820, 1990.
[h] A. Della Ratta, J. Melngailis, and C. V. Thompson, *J. Vac. Sci. Technol.*, **B11:** 2196, 1993.
[i] H. Komano, Y. Ogawa, and T. Takigawa, *Jpn. J. Appl. Phys.*, **28,** 2372, 1989.
[j] A. N. Campbell et al., 23rd International Symposium for Testing and Failure Analysis, 1997.
[k] R. J. Young and J. Puretz, *J. Vac. Sci. Technol.*, **B13:** 2579, 1995.
[l] K. Edinger, J. Melngailis, and J. Orloff, *J. Vac. Sci. Technol.*, **B16**: 3311, 1998.

material deposited so that the net deposition yield is determined by the difference between the dissociation yield and the milling yield.

The gas usually adsorbs as a monolayer, and for optimum deposition the gas supply should exceed the rate at which it is dissociated by the ion beam. This is usually the case if the beam is scanned rapidly over some area. To obtain a maximum deposition rate and to have conditions for quoting a consistent net deposition yield, one should operate in the ion-beam-limited mode rather than the gas-supply-limited mode. Some of the gases and deposits are shown in Table 2.

Because the precursor gases generally contain carbon, the deposits also contain some carbon. In addition, of course, gallium is also implanted into the deposited material. As a result the resistivity of the "metal" films is considerably higher than that of pure bulk metals. Unfortunately, deposition from non-carbon-containing precursors such as WF_6 has not worked with Ga^+ ions; etching rather than deposition is produced. (As shown in the table, tungsten has been deposited from WF_6 using relatively low-energy Ar^+ ions.) For both gold and copper the carbon content in the film and the resistivity can be greatly reduced by heating the substrate to 80°C to 100°C during deposition (see Table 2) This is presumably due to the fact that the organic reaction products desorb more readily from the surface and are not further broken down by the ion bombardment (14,15).

The detailed mechanism of ion-induced deposition is believed to be substrate mediated. As in the case of sputtering, the incident ions create collision cascades, some of which come to the surface. If these collision cascades impart an energy larger than the surface binding energy (~4 eV for most materials) to the surface atom, it will be sputtered, but if the collision cascades impart an energy greater than the dissociation energy

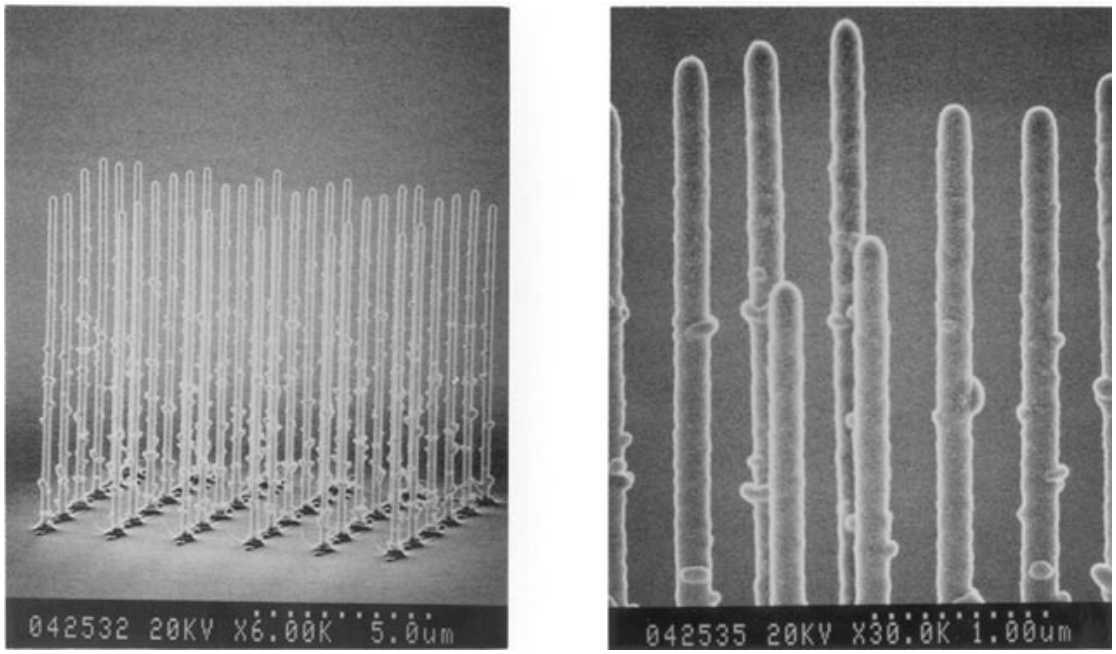

Fig. 8. High-aspect-ratio gold posts (∼150 nm diameter) deposited by stepping the ion beam in a 6 × 6 grid. From P. G. Blauner, IBM Watson Research Laboratories.

to adsorbed molecules, the molecules will break up (16,17). In the case of the gold precursor, this energy is ∼1 eV. This model has been used to predict the dissociation yield and correlates fairly well with measurements (16,17) over a range of ion masses (He to Xe) and ion energies (2 keV to 100 keV).

In a number of applications insulator deposition is desirable. Various silicates have been used, sometimes mixed with O_2 (see Table 2). The oxide quality is far from that of pure SiO_2; typical resistivities range from 10^7 Ω·cm to 10^8 Ω ·cm (compared to 10^{12} Ω·cm to 10^{16} Ω·cm for pure SiO_2). Still these oxides are useful as insulators between metal layers in integrated circuits.

Deposition occurs when the ion beam is incident. Thus deposits of dimensions comparable to the beam diameter should be possible. So far the smallest dimension deposits made are of the order of 100 nm to 150 nm, in spite of the fact that beam diameters considerably smaller are available (18). Presumably this is due to the nonlocal ion–adsorbate interaction. Nevertheless some high aspect ratio structures have been deposited (see Fig. 8).

Ion-Beam-Assisted Etching. In the ion-assisted etching process a reactive gas, such as Cl_2 or XeF_2, which by itself does not react with the substrate, is introduced using a capillary feed as shown in Fig. 2. However, where the focused ion beam is incident, a reaction is induced and material is removed with a yield of typically 10 times higher than by sputtering alone. Some of the gas–substrate combinations are listed in Table 3. One other feature of ion-assisted etching is selectivity. For example, to etch Al, which is deposited as a film on SiO_2, one would use Cl_2, since it enhances the removal rate of Al by 10 but does not enhance the removal rate of SiO_2. Another interesting etch gas is water (19). It enhances the etch rate of organic films such as polyimide or PMMA by about 20 ×, but it *depresses* the etch rate of Si, SiO_2, or Al by factors of 3 to 5. The depressed etch rate may be due to the fact that the H_2O reoxidizes the material as it is being milled. Incidentally, H_2O also enhances the etch rate of diamond by about 10 times.

Table 3. Ion-Beam-Assisted Etching

Substrate	Ion (Energy)	Gas Flux (or Pressure on Substrate)	Etching Rate Enhancement (rate with gas/rate without gas)	Reference
Si	35 keV (Ga)	Cl_2 (4 mTorr)	20	(*a*)
InP	35 keV (Ga)	Cl_2 (1.3 mTorr)	20–30 (140°C)	(*a*)
SiO_2	50 keV (Ar)	XeF_2 (20 mTorr)	100	(*b*)
W	20 keV (Ga)	XeF_2 2 Torr	15–75	(*c*)
Al		Cl_2	5–10	(*d*)
PMMA	25 keV (Ga)	H_2O (70 mTorr)	20	(*e*)
Diamond	25 keV (Ga)	H_2O (70 mTorr)	10	(*e*)
Si	25 keV (Ga)	H_2O (70 mTorr)	0.3	(*e*)

[a] Y. Ochiai et al., *J. Vac. Sci. Technol.*, **B5:** 423, 1997.
[b] Z. Xu, K. Gamo, and S. Namba, *J. Vac. Sci. Technol.*, **B6:** 1039, 1998.
[c] R. R. Kola, G. K. Celler, and L. R. Harriott, MRS Symposium, Beam-Solid Interaction: Fundamentals and Applications, M. A. Nastasi et al., (eds.), 1993, Vol. 279, p. 593.
[d] J. D. Casey et al., *Microelectronic Eng.* **24:**43, 1994.
[e] T. J. Stark et al., *J. Vac. Sci. Technol.*, **B13:** 2565, 1995.

Ion-assisted etching is not as widely used or developed as milling or deposition. However, it is quite important for rapid material removal, for selectivity, and for forming deep, high-aspect-ratio structures in which redeposition has to be avoided.

Applications of Focused Ion Beams

The focused ion beam is most widely used when small quantities of material need to be removed or added with great precision. Although many applications have been demonstrated, (20) the main ones in microelectronics are circuit failure analysis, circuit rewiring, transmission electron microscope (*TEM*) sample preparation, and disk drive head trimming.

Failure Analysis. When a failure such as a nonfunctioning transistor or an open contact is identified in an integrated circuit, it can be examined and analyzed using focused ion-beam sectioning. Using the scanning ion microscope mode and the circuit layout information, the faulty site is positioned under the focused ion beam. A pit is milled into the circuit with the defect site as one wall. The pit has to be deep enough and large enough so that the defect can be seen in a tilted sample either with the ion beam or with an SEM. (In some instruments the SEM is built into the same chamber as the *FIB* and one can section and "look" at the same time.) The pit is usually milled with a coarse beam of a few nanoamperes current. Then the current is reduced to achieve a finer focus and closely controlled sectioning near the defect [see Figure 9(a)]. One can, of course, make successive cuts through the defect to see different cross sections. An example of a sectioned device is shown in Fig. 9(b)).

How long does it take to mill out the material? Assume the material is Si and the milling yield is 3 atoms/ion (Table 1). Si has a density of 5×10^{10} atoms/μm^3. So 1.7×10^{10} ions are needed to remove 1 μm^3. A 5 nA beam delivers 3.1×10^{10} ions/s and will remove 1 μm^3 of Si in 0.53 s. Thus, a sloping pit 10 m $\times$ 50

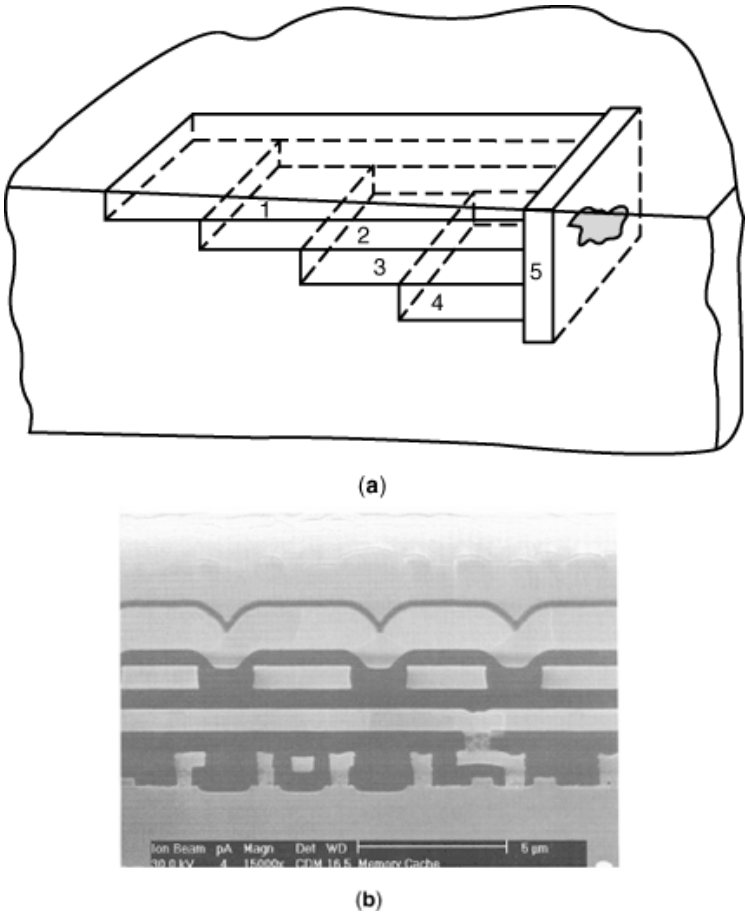

Fig. 9. (a) Schematic of the milling out of a staircase pit to reveal a defect on the right wall. The milling is carried out by removing the volumes 1–5 in order. Number 5 is the final mill usually done with a finer beam. (b) Example of a milled-out cross section.

m which is 10 μm^3 deep at the sectioned end would take 22 min to mill in Si. If a reactive gas is used, such as Cl_2, the Si removal rate can be increased by a factor of up to 20 (see Table 3), and the time to mill the pit is reduced to under 1 min. Since a device is typically made up of slices of different materials, such as SiO_2, Al, and Si, different reactive gases would in principle be needed to optimize the material removal rate. With or without gas enhancement the removal rate in most cases is not unreasonable since the information gained is valuable. Alternative methods such as cutting with a diamond saw and sectioning the entire device are far more difficult and in most cases would not be able to guarantee that the cross section will intersect the defect.

Circuit Rewiring. When an integrated circuit with millions of transistors is being designed, and the first prototype is built, it may have errors, and the device may not function. The *FIB* provides a tool for correcting some errors so that at least the prototype can be tested. This is very valuable since the alternative is to make one or more new masks in the mask set and refabricate the device, a long, complex and expensive process.

Since integrated circuits may have several levels of metal film conductors, the rewiring process can be demanding. If a conductor needs to be cut that is close to the surface, a small trench can simply be milled across it to break the metal connection. If a connection needs to be made between two metal films, via holes are first

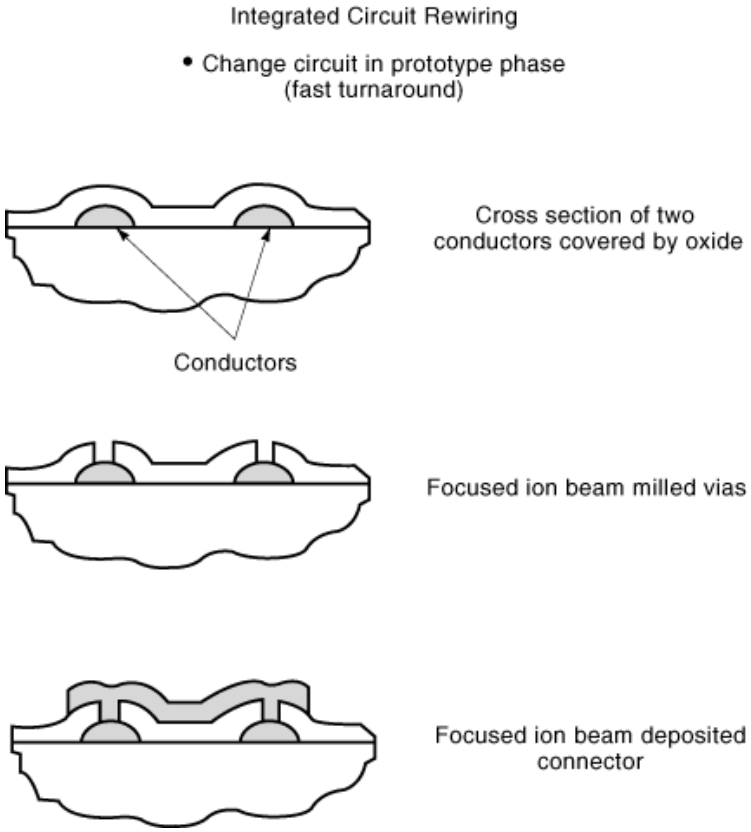

Fig. 10. Schematic of a rewiring process where vias are first milled down to the two underlying metal "wires." Using *FIB*-induced deposition, the wires are connected.

milled through the covering oxide film to expose the metal, and then using a metal bearing precursor gas (see Table 2) a conductor is deposited from one via to the other, as shown schematically in Fig. 10 and on a real device in Fig. 11. Since, as shown in Table 2, oxides can also be deposited with fairly good insulating qualities, more elaborate repairs are also possible. For example, a metal connection may need to be made to a lower level that is covered by another metal layer. In that case a larger via hole is milled through the upper level of metal down to the lower level, then the via is filled with oxide, a new smaller via is milled through the refilled oxide, and metal is deposited down to the lower level, as shown in Figs. 12(a) and 12(b). These cutting and deposition procedures are useful not only for rewiring integrated circuits so they can operate but also for operating test sites on the circuit so that signal levels can be measured at specific sites either by electron-beam testing or by mechanical probing. For the latter case a probe pad of metal may need to be deposited on the top surface of a circuit. Note that the resistivity of the deposited "metal" (Table 2) is often many times higher than that of pure metal. This shortcoming is not serious, since the length of the conductors deposited is not large and, if need be, the deposit can be made thicker to reduce the resistance.

TEM Sample Preparation. In spite of the progress in increasing the resolution of the *FIB* in the scanning ion microscope as well as the resolution of scanning electron microscopes (*SEMs*), the transmission electron microscopes (*TEMs*) still have the highest resolution and can provide additional information, such as crystal structure. The preparation of samples, often slivers less than 100 nm thick, cut from the interior of

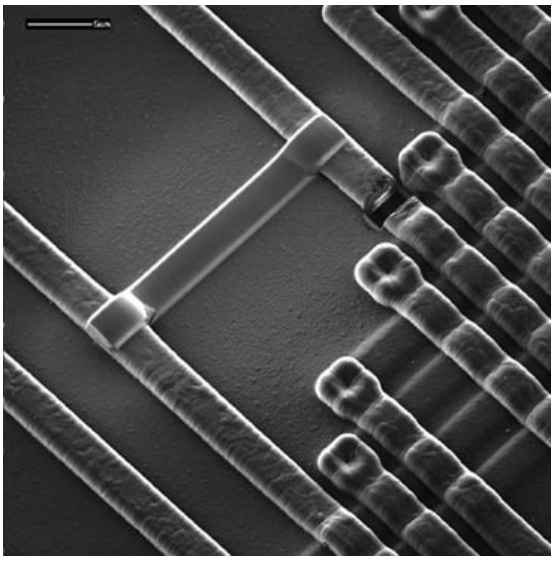

Fig. 11. An example of a cut in a wire and a deposited connector (from FEI Co.).

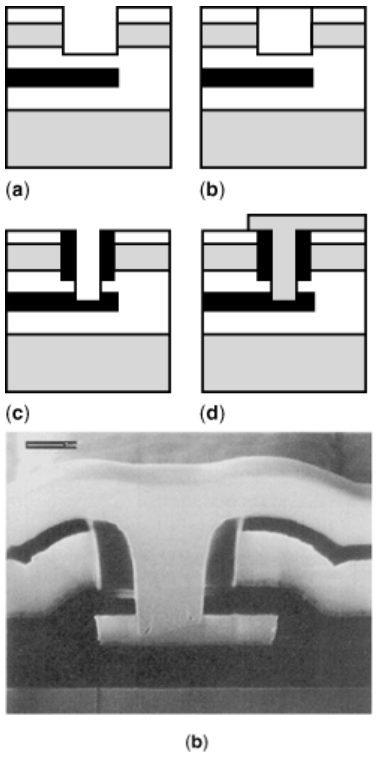

Fig. 12. (a) Schematic showing how a connection is made to a lower-level metal through an upper level metal. A large via is first milled through the upper level, filled with SiO_2, and then a smaller via is milled to the lower metal and filled with metal. (b) Cross section of an actual filled via fabricated as in (a).

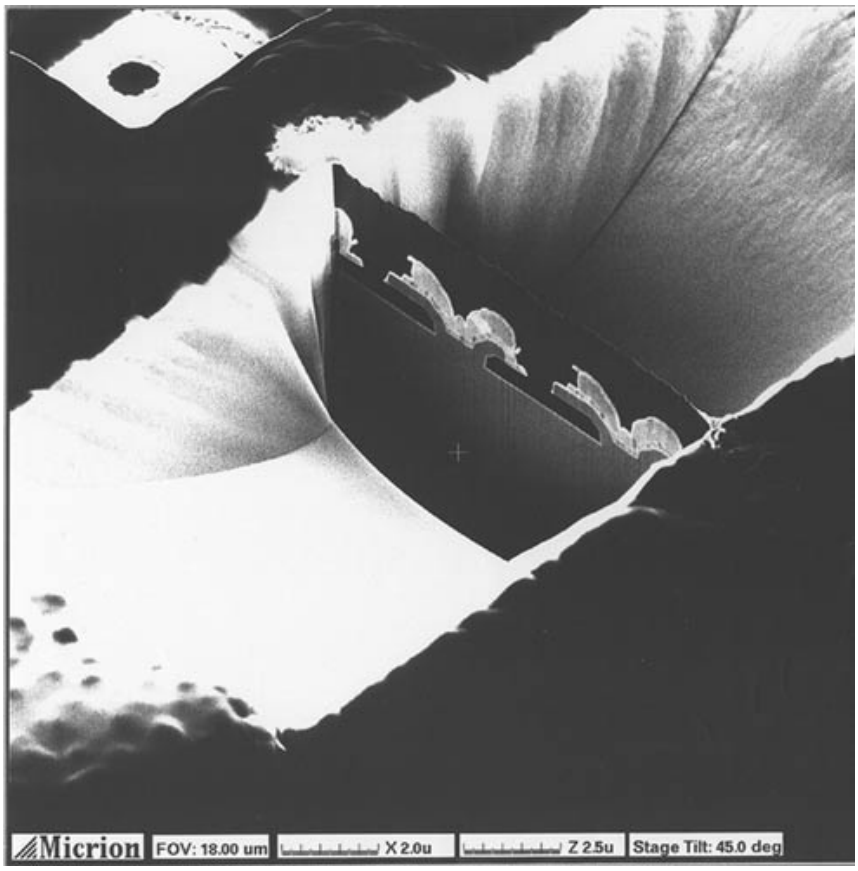

Fig. 13. Example of a TEM sample created by milling two pits on either side of the sample. The final thinning of the sample is done with a fine beam. The snowlike material on the edges of the pits is due to redeposition.

a circuit or other material by conventional methods is time consuming and often has a low success rate. The sample has to be potted, sliced, polished, and finally thinned by angled broad-beam ion milling. It is often difficult to make the cross section sliver in a desired location in the material. With the *FIB*, on the other hand, the exact location can be determined as long as there is a specific top surface feature that one can align on. The procedure for making the TEM sample is similar to the failure analysis procedure in Fig. 9, except that two pits are milled one on each side of the sample. The final sliver is then carefully milled with a very fine beam to leave a thin <0.2 μm thick "wall" as shown in Fig. 13. This wall is then cut free with the ion beam by tilting the sample and milling through the bottom and two sides. The membrane can then be picked up by touching it with a finely pointed, drawn pyrex fiber, and placed on a TEM grid (21). Membranes less than 50 nm thick have been prepared and lattice plane images observed. The TEM sample could also be examined without this lift-out procedure, but then a lot more material has to be cut away to provide a clear line of sight so that the electrons in the TEM can pass through the sample.

Trimming of Magnetic Disk Drive Reading–Writing Heads. The density of data storage in disk drives is partly determined by the dimensions of the poles on the head. The part of the head that faces the disk consists of two poles of an electromagnet for writing, that is locally changing the direction of magnetization and a sensitive magnetoresistive element for reading, as shown in Fig. 14(a). The narrower the head, the closer the tracks on a magnetic disk can be spaced together. Conventional lithography can be used to define the width of

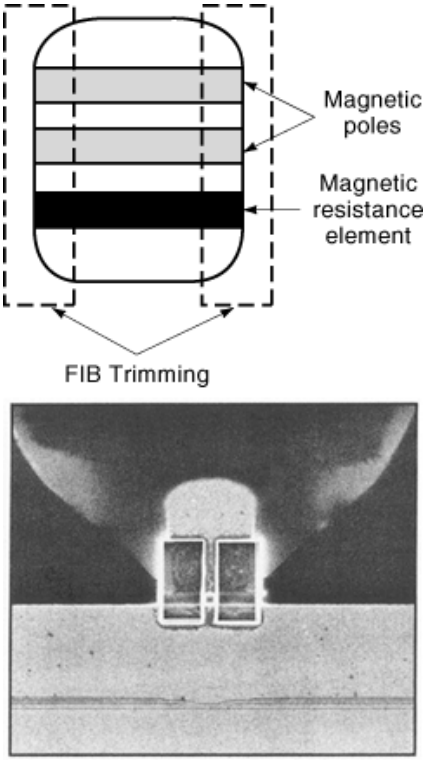

Fig. 14. (a) Schematic of the magnetic disk head as seen from the disk being read. The area to be trimmed off by the *FIB* is shown by the dotted rectangles. (b) A photograph of a milled disk head.

the head, but because of the multimaterial, three-dimensional character of the head, this is difficult to do with submicrometer precision. *FIB* milling is uniquely suited to trim the width of the heads with ~10 nm precision. In addition the *FIB* offers complete flexibility and is useful during development to determine what geometry works best. A trimmed head is shown in Fig. 14(b).

Other Applications. The four previous applications are probably the most widely practiced. Others are as follows.

(1) *Mask Repair.* All integrated circuits are "printed" using a mask to expose resist. The mask in optical lithography consists of a quartz plate with the image of one layer of the chip circuit defined by a pattern of opaque metal covered regions and of transparent regions. This pattern is demagnified (usually about 4 ×) and projected on to a silicon wafer. The mask may have millions of features and often some features may be defective, that is, missing or unwanted metal film. The *FIB* can be used to remove metal or other unwanted absorber or to deposit missing absorber. This was the earliest successful application of *FIB* commercially and may again become critically important when optical lithography is replaced by some other technique, such as proximity printing, X-ray and soft X-ray projection (also called EUV, extreme ultraviolet), electron-beam projection, and ion-beam projection. In all of these cases the mask technology is much more demanding than the metal on quartz and the mask repair will require the fine-resolution capability of the *FIB* (22).

(2) *Tunneling Microscopy Tips.* The *FIB* can be used to sharpen or otherwise shape the fine tips used in various forms of tunnel microscopy. Since the tips have a distinct three-dimensional character compared to a pit in a surface, the shaping of the tips is more challenging (23).

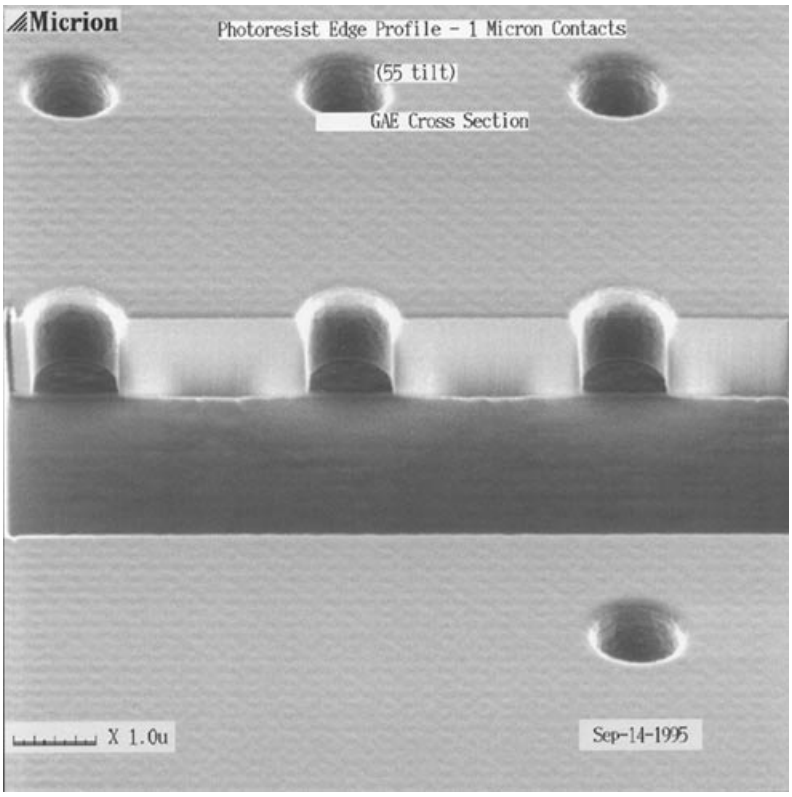

Fig. 15. Via holes defined in resist. The central three have been sectioned by gas assisted etching. The resist profile for the unsectioned vias is clearly difficult to determine.

(3) *Semiconductor Laser Facets.* The ends of a semiconductor laser have to be parallel "mirrors" and are usually formed by cleaving along crystal axis. This, however, restricts the geometry. The mirrors have also been successfully cut using *FIB* milling, without degrading the efficiency or threshold current (24,25).

(4) *High-Temperature Superconduction Josephson Junctions.* The high-temperature superconducting materials, such as (*YBCO*) yttrium–barium–copper–oxide compounds as well as the substrates on which they are grown, such as $LaAlO_3$, are difficult to pattern by conventional techniques. *FIB*s can mill any material and have been used to successfully fabricate Josephson junctions (26).

(5) *Secondary-Ion Mass Spectrometry.* Secondary-ion mass spectrometry is a well-known analysis technique in which material is sputtered and the ions sputtered off are analyzed in a mass spectrometer, thereby identifying the constituents of the substrate. By using a focused ion beam to mill the substrate this identification can be carried out with submicrometer resolution (see Ref. 8).

(6) *Sectioning of Resist.* As dimensions in integrated circuits shrink, the resist features have higher and higher aspect ratios, and the geometry of the resist sidewalls becomes more critical. In addition, it is difficult to see the bottom of deep resist features using an SEM. The resist structures need to be cross sectioned to be examined by SEM. The *FIB* with water vapor as an etch gas is very effective in sectioning resist because it increases the removal rate of the organic material (resist) by as much as a factor of 20 while reducing the milling rate of the underlying material, such as Si or SiO_2 by a factor of 3 to 5 (see Ref. 19). Thus resist can be cross sectioned clearly with little or no redeposition and minimal etching of the underlying substrate. An example of a resist cross section obtained by *FIB* is shown in Fig. 15. The preparation of samples for

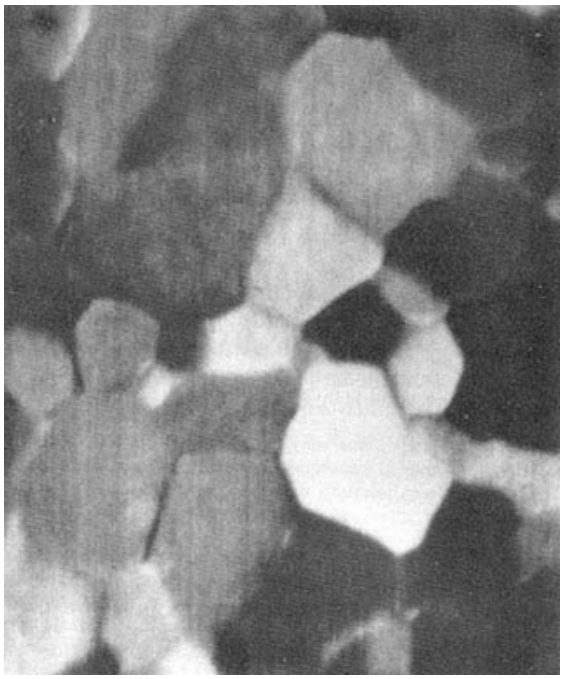

Fig. 16. Al (0.5% Cu) film imaged with 70 keV Ga^+ ions. Field size is 11 × 11 μm (from Ref. 27). The secondary-electron emission is a strong function of angle. If the sample is tilted, say 5° or 10°, the contrast changes radically. Imaging at a few angles is used to unambiguously identify the crystal grains.

SEM observation can be used in other circumstances as well. (See also the previous section titled "Failure Analysis.")

(7) *Examining Crystal Structure.* As mentioned earlier the penetration of ions into a crystal depends on the orientation of the crystal axis relative to the incident beam direction. Thus also the secondary-electron emission coefficient will vary as a function of orientation, and in a polycrystalline film each grain will appear of a different contrast (27,28). An example is shown in Fig. 16. The ability to examine grain structure is particularly useful when combined with *FIB* sectioning. Thus, for example, one can examine the crystal structure in a conducting interlevel connector plug (usually called a via) by first sectioning it and then looking at the grain structure.

The applications summarized here are being implemented in the microelectronics industry. Other applications of *FIB*s may well develop in the future.

Future Applications

Micro-Electro-Mechanical Systems. As micro-electro-mechanical systems (*MEMS*) develop the unique capabilities of *FIB*s to remove and add material with nanometer resolution, albeit slowly, is likely to be useful. For example, an *FIB* has been used to cut a miniature gap in an accelerometer structure (29). The machining of the disk heads could also be regarded as a MEMS application.

Implantation. Focused ion-beam implantation provides unprecedented flexibility to fabricate unique semiconductor devices. The dose of ions can be controlled point by point with 50 nm resolution in a maskless,

resistless process. This permits devices to be made side by side, each with different implant doses, or it permits lateral gradients of doping to be generated within a device. In addition, when combined with local ion-induced deposition we can envisage devices made entirely by *FIB*s with no lithography. This would permit simple circuits to be built literally on the side of a needle or on other nonplanar geometrics. The machines used for implantation in general use alloy sources such as Pd/As/B or Au/Si/Be instead of the Ga used for all of the practical applications discussed previously. Thus the systems are more complicated and have to include a mass filter as shown in Fig. 2.

So far the applications of implantation have been demonstrated as part of conventional fabrication by substituting *FIB* implantation for broad-area, lithographically defined implantation. Some examples are a fast 1 GHz flash analog-to-digital converter made by implanting 32 transistors each with a different dose to yield different threshold voltages (30), transistors with doping gradients in the channel (31), tunable Gunn diodes (32), or faster charge-coupled devices (33). So far these are research results and have not found their way into production because the *FIB* implantation is slow, the alloy sources are hard to use and are not as reliable as the Ga^+ sources, and, in some cases, once the advantage of a certain geometry is demonstrated by *FIB* implants, ways to achieve the same result with modifications of conventional processes have been found. Nevertheless, many *FIB* implanted devices are unique, and the fabrication time is not prohibitive as long as the number of special transistors on a chip is small, that is, hundreds, not millions. With a 30 pA beam, a dose of 10^{12} ions/cm^2, typical of transistor and channel implants, can be delivered over 1 mm^2 in 50 s. In addition, the ability to fabricate devices on unique geometries has not been explored. The need to do this may increase as the development of MEMS progresses.

Summary

The number of *FIB* systems with Ga^+ ions in use numbers in the many hundreds and is increasing, mainly due to the applications in the microelectronics industry. Given the unique nanometer scale material removal, addition, and modification capabilities of *FIB*s new applications will also likely emerge.

BIBLIOGRAPHY

1. R. L. Seliger W. P. Fleming, *J. Vac. Sci. Technol.* **10**: 1127, 1973; *J. Appl. Phys.*, **45**: 1416, 1974.
2. R. Clampit, K. L. Aitkent, D. K. Jeffries, *J. Vac. Sci. Technol.*, **12**: 1208, 1975; R. Clampit D. K. Jeffries, *Nucl. Instrum. Methods*, **149**: 739, 1978.
3. V. E. Krohn G. R. Ringo, *Appl. Phys. Lett.*, **27**: 479, 1975.
4. L. W. Swanson, *et al. J. Vac. Sci. Technol.*, **16**: 1864, 1979.
5. R. L. Seliger, *et al. Appl. Phys. Lett.* **34**: 510, 1979.
6. J. Orloff (ed)., *Charged Particle Optics.* Boca Raton, FL: CRC Press, 1997.
7. P. O. Prewett L. L. R. Mair, *Focused Ion Beams from Liquid Metal Ion Sources*, Taunton, Somerset, England: Research Studies Press, Wiley, 1991.
8. R. Levi-Setti, *Advances in Electronics and Electron Physics*, Suppl. 13A, New York: Academic, 1980, 261.
9. J. F. Ziegler, J. P. Biersack, V. Littmark, *The Stopping and Range of Ions in Solids*, Vol. 1, New York: Pergamon, 1984. (The TRIM program is updated every year.)
10. J. F. Ziegler, Ion implantation physics, in J. F. Ziegler (ed.), *Handbook of Ion Implantation Technology*, Amsterdam: North Holland, 1992, p. 15.
11. H. H. Anderson H. L. Bay, Sputter yield measurements, in R. Behrisch (ed)., *Sputtering by Particle Bombardment I, Physical Sputtering of Single Element Solids*, Berlin: Springer Verlag, 1981.
12. D. Santamore, *et al. J. Vac. Sci. Technol.*, **B15**: 2346, 1997.
13. X. Xu, *et al. J. Vac. Sci. Technol*, **B10**: 2675, 1992.

14. P. G. Blauner, *et al. J. Vac. Sci. Technol.*, **B7**: 1816, 1989.
15. A. D. Della Ratta, J. Melngailis, C. V. Thompson, *J. Vac. Sci. Technol.*, **B11**: 2195, 1993.
16. A. D. Dubner, *et al. J. Appl. Phys.*, **70**: 665, 1991.
17. J. S. Ro, C. V. Thompson, J. Melngailis, *J. Vac. Sci. Technol.*, **B12**: 73, 1994.
18. P. G. Blauner, IBM Watson Laboratory, private communication.
19. T. J. Stark, *et al. J. Vac. Sci. Technol.*, **B13**: 2565, 1995.
20. For a recent review of the applications, see F.A. Stevie et al., *Surf. Interface Anal.*, **23**: 61–68, 1995.
21. M. H. F. Overwijk, F. C. Van der Heuvel, C. W. T. Bulle-Lieuwma, *J. Vac. Sci. Technol.*, **B11**: 2021, 1993.
22. P. G. Blauner, *J. Vac. Sci. Technol.*, **B13**: 3070, 1995.
23. M. J. Vasile, C. Biddick, S. A. Schwalm, *J. Vac. Sci. Technol.*, **B12**: 2388, 1994.
24. L. R. Harriott, *et al. Appl. Phys. Lett.*, **48**: 1704, 1986.
25. J. Puretz, *et al. Electron. Lett.*, **22**: 700, 1986.
26. C. H. Chen,, *et al. Appl. Phys. Lett.*, **73**: 1730, 1998.
27. K. Nikawa, *J. Vac. Sci. Technol.*, **B9**: 2566, 1995.
28. D. L. Barr, L. R. Harriott, W. L. Brown, *J. Vac. Sci. Technol.*, **B10**: 3120, 1992.
29. J. B. Daniel, *et al.* Micro and Nano Engineering Conf., Glasgow, Scotland, 1996.
30. J. Y. Lee R. L. Kubena, *Appl. Phys. Lett.*, **48**: 668, 1986; R. H. Walden et al., *Proc. IEEE 1988, Custom Integrated Circuits Conf.*, 1988, IEEE 88 CH 2584–1, p. 18.7.1.
31. A. F. Evason, J. R. A. Cleaver, J. Ahmed, *IEEE Electron Dev. Lett.*, **9**, 281, 1988; C.-C. Shen et al., *IEEE Trans. Electron De- vices*, **45**: 453–459, 1998.
32. H. J. Lezec, *et al. IEEE Electron Device Lett.*, **9**: 476, 1988.
33. A. L. Lattes, *et al. IEEE Trans. Electron Devices*, **39**: 1772–1774, 1992.

JOHN MELNGAILIS
University of Maryland
LYNWOOD W. SWANSON
FEI Co.
WILLIAM THOMPSON
Micrion Corp.